

---

# Deep Discriminative Direct Decoders for High-dimensional Time-series Analysis

---

Mohammad R. Rezaei<sup>1,2,5</sup>, Milos R. Popovic<sup>2,5</sup>, Milad Lankarany<sup>1,2,3,5\*</sup>, Ali Yousefi<sup>4\*</sup>

<sup>1</sup>Krembil Brain Institute, University Health Network, Toronto, Canada.

<sup>2</sup>KITE Research Institute, Rehabilitation Institute, University Health Network, Toronto, Canada.

<sup>3</sup>Department of Physiology, University of Toronto, Toronto, Canada.

<sup>4</sup>Worcester Polytechnic Institute (WPI), Worcester, MA, USA.

<sup>5</sup>Institute of Biomedical Engineering University of Toronto, Toronto, Canada.

\*Corresponding authors: milad.lankarany@uhnresearch.ca, ayousefi@wpi.edu

## Abstract

Dynamical latent variable modeling has been significantly invested over the last couple of decades with established solutions encompassing generative processes like the state-space model (SSM) and discriminative processes like a recurrent or a deep neural network (DNN). These solutions are powerful tools with promising results; however, surprisingly they were never put together in a unified model to analyze complex multivariate time-series data. A very recent modeling approach, called the direct discriminative decoder (DDD) model, proposes a principal solution to combine SMM and DNN models, with promising results in decoding underlying latent processes, e.g. rat movement trajectory, through high-dimensional neural recordings. The DDD consists of a) a state transition process, as per the classical dynamical models, and b) a discriminative process, like DNN, in which the conditional distribution of states is defined as a function of the current observations and their recent history. Despite promising results of the DDD model, no training solutions, in the context of DNN, have been utilized for this model. Here, we propose how DNN parameters along with an optimal history term can be simultaneously estimated as a part of the DDD model. We use the D4 abbreviation for a DDD with a DNN as its discriminative process. We showed the D4 decoding performance in both simulation and (relatively) high-dimensional neural data. In both datasets, D4 performance surpasses the state-of-art decoding solutions, including those of SSM and DNNs. The key success of DDD and potentially D4 is efficient utilization of the recent history of observation along with the state-process that carries long-term information, which is not addressed in either SSM or DNN solutions. We argue that D4 can be a powerful tool for the analysis of high-dimensional time-series data without the burden of building intricate conditional models for individual observations, with other promising attributes like low-computational cost in its decoding step.

## 1 Introduction

Dynamical latent variable modeling has been widely used in characterizing multivariate time-series data[16], including neural recordings[22, 2, 11, 12, 26]. For time-series data analysis, two widely used modeling solutions are, a) state-space models (SSM)[1], and b) neural networks including recurrent neural networks (RNN)[5, 13] and deep neural networks (DNNs)[17, 27, 23, 21, 6]. These solutions have been successfully applied in many applications; however, each solution is built upon prior assumptions that make their applications in certain time-series data challenging[24]. In SSMs, we build a) a state process, that characterizes how the latent process(es) evolve over time,

and b) an observation process, that represents the conditional distribution of observed signal given the state process. SSMs like any generative model require proper probabilistic models to characterize how the state process evolves over time, and how the observed data is generated given the state process. Building these models is challenging for high-dimensional observation processes, except we build a simplified observation model that leads to a biased or inaccurate inference. Furthermore, the assumption of conditional independence of the current observation from its previous time points given the state process might not hold in many time-series data. The recursive filter solution in SMMs considers this assumption; otherwise, the inference solution in SMMs becomes computationally intractable[10].

DNNs and RNNs are deemed to address most of the challenges present in SMMs; however, these models are not designed to incorporate information at different timescales carried by the state and observation processes. This will limit applications of discriminative processes, like DNN and RNNs, in the inference of complex and intertwined dynamics. A critical advantage of SMMs is the way the state and observation processes at different timescales are combined in the characterization of data and inference step. Critical advantages of DNNs and RNNs are their precision power and scalability. A new variant of SMM that has been recently introduced, called the direct discriminative decoder (DDD) model suggests a modeling pipeline to merge the advantages of SMM and DNN in a unified modeling framework [18]. If the promises of DDD hold, we aim to expand its utilities in decoding complex and high-dimensional time-series data by embedding DNN and RNN in DDD. The DDD then consists of a state transition process, as per SSMs, and a discriminative process in which the conditional distribution of the state,  $\mathbf{x}_k$ , is defined as a function of the current current observation,  $\mathbf{s}_k$ , and a subset of observations from previous time points  $\mathbf{h}_k$ . The filter solution in the DDD model is defined by

$$p(\mathbf{x}_k|\mathbf{s}_{1,\dots,k}) \propto \frac{p(\mathbf{x}_k|\mathbf{h}_k, \mathbf{s}_k)}{p(\mathbf{x}_k|\mathbf{h}_k)} \int p(\mathbf{x}_k|\mathbf{x}_{k-1})p(\mathbf{x}_{k-1}|\mathbf{s}_{1,\dots,k-1})d\mathbf{x}_{k-1} \quad (1)$$

Where the nominator of the first term is called the prediction process and the denominator, using Chapman-Kolmogorov equation[14] to expand  $p(\mathbf{x}_k|\mathbf{h}_k) = \int p(\mathbf{x}_k|\mathbf{x}_{k-1})p(\mathbf{x}_{k-1}|\mathbf{h}_{k-1}, \mathbf{s}_{k-1})d\mathbf{x}_{k-1}$ , called one-step prediction density by the prediction process from last time-step. Here  $p(\mathbf{x}_k|\mathbf{x}_{k-1})$  represents the state transition process and  $\mathbf{h}_k = \{\mathbf{h}_{k-1}, \mathbf{s}_{k-1}\}$ . The second term in the right side of equation 1 is the one-step prediction density by the posterior function from the last time-step defined by the Chapman-Kolmogorov equation. The DDD incorporates the advantages of SMM, a structure to incorporate information from slow timescales that present signals, and machine learning (ML) approaches to build expressive models using DNN and RNNs. [18] and [3] showed the DDD performance precedes state-space and RNN models in both simulation and real data. However, DDD utility and learning were only demonstrated using simple discriminative models like the generalized linear model (GLM). The proposed learning solution for the DDD model is restrictive, given the denominator term contribution in parameter estimation is being ignored. In this research, we propose two learning solutions for the DDD model including those with a DNN as its prediction process – we call a DDD with a DNN prediction process, D4. For the learning step, we derive a tight lower bound for the full log-likelihood of the state and observation and derive how DNN elements model including DNN parameters and history term can be learned. We demonstrate D4’s performance in both simulation and real data and compare its result with DNN and SSM models. For the real-world application, we use the D4 model to decode 2-D trajectories of a rat moving through a maze from the ensemble spiking activity of its hippocampus place cells, 62 cells[19]. The DDD and D4 can be applied to a broader class of time-series analysis where the connection between high-dimensional observation and the underlying process is complex and is not known firsthand. These models can scale efficiently to high-dimensional data and they can be applied to many modalities of observed data including continuous, discrete, and or a mixture of them.

## 2 Methods

Let’s assume we have  $\mathbf{s}_k \in \mathbb{R}^N$  for  $k = 1$  to  $K$ , from a time series data. We also assume there is a latent process,  $\mathbf{x}_k$  for every time index  $k$ . The state transition process at time index  $k$  is defined by

$$\mathbf{x}_k|\mathbf{x}_{k-1} \sim g(\mathbf{x}_{k-1}; \boldsymbol{\omega}) \quad (2)$$

where  $\boldsymbol{\omega}$  is the set of free parameters of the state equation. Here we expect that the observation at each time index is high-dimensional and possibly non-linear function of the latent state. The prediction

process of the D4 is defined by

$$\mathbf{x}_k | \mathbf{s}_k, \mathbf{h}_k \sim f(\mathbf{s}_k, \mathbf{h}_k; \Omega) \quad (3)$$

where  $\mathbf{h}_k$  is the history term at time index  $k$  comprised of the observation from previous time points, and  $\Omega$  is the model free parameters. The inference in the D4 is defined by equation 1. Our learning objective is to find a set of parameters that maximizes the likelihood over the joint distributions of state variables and observations,  $\{\mathbf{x}_k, \mathbf{s}_k\}_{k=1}^K$ .

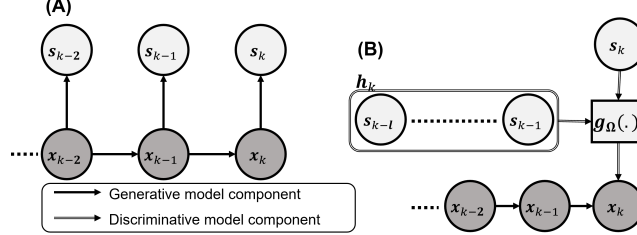


Figure 1: Graphical representation of the D4 model. A) SSM , B)D4 models.  $g_{\Omega}(\cdot)$  is the prediction process, possibly, a DNN, parameterized by  $\Omega$ . Further explanations of the DDD graph can be found in [18] and  $l$  is the maximum length of the history term.

## 2.1 Parameter estimation in D4 model

Given having latent variables in the model, we use EM algorithm [7]. The expected value of log-likelihood function,  $Q$ , is defined by  $Q$  as

$$Q(\theta | \theta^{(r)}) = \mathbb{E}_{\mathbf{x}_{0:K} | \mathbf{s}_{1:K}; \theta^{(r)}} [\log(p(\mathbf{x}_0; \omega_0) \prod_{k=1}^K p(\mathbf{x}_k | \mathbf{x}_{k-1}; \omega) \prod_{k=1}^K \frac{p(\mathbf{x}_k | \mathbf{s}_k, \mathbf{h}_k; \Omega)}{p(\mathbf{x}_k | \mathbf{h}_k; \Omega)})] \quad (4)$$

where  $\theta^r = \{\Omega^r, \omega^r\}$  represents model parameters estimated by maximizing  $Q$  from the previous iteration of EM algorithm, M-step[18]. For the simplicity of notation, we use  $\mathbb{E}_K$  for  $\mathbb{E}_{\mathbf{x}_{0:K} | \mathbf{s}_{1:K}; \theta^{(r)}}$  in the rest of the paper. We can expand the  $Q(\theta | \theta^{(r)})$  function, which gives

$$Q(\theta | \theta^{(r)}) = \mathbb{E}_K [\log p(\mathbf{x}_0; \omega_0) + \sum_{k=1}^K \log p(\mathbf{x}_k | \mathbf{x}_{k-1}; \omega) + \sum_{k=1}^K \log p(\mathbf{x}_k | \mathbf{s}_k, \mathbf{h}_k; \Omega)] - \mathbb{E}_K [\sum_{k=1}^K \log p(\mathbf{x}_k | \mathbf{h}_k; \Omega)] \quad (5)$$

For the cases where the state process is linear with additive Gaussian noise and the prediction process is a multi-variate normal, we can find a closed-form solution for different terms of the  $Q$  function. When the noise characteristics in the prediction process is defined as a function of the observation or the state transition is nonlinear, it will be hard to find a closed-form solution for the  $Q$  function. It is possible to use sampling techniques to calculate the expectation for the first term; however, finding the expectation for the last term is challenging given it involves a second integration over the state. Instead, we show that we can find an approximation for the last term which turns into a lower bound for the  $Q$ . We can write the last term in  $Q$  as

$$\begin{aligned} \mathbb{E}_K [\sum_{k=1}^K \log p(\mathbf{x}_k | \mathbf{h}_k; \Omega)] &= \sum_{k=1}^K \int p(\mathbf{x}_k | \mathbf{s}_{1:K}, \theta^{(r)}) \log p(\mathbf{x}_k | \mathbf{h}_k; \Omega) d\mathbf{x}_k = \\ &= \sum_{k=1}^K \int p(\mathbf{x}_k | \mathbf{s}_{1:K}, \theta^{(r)}) \log \frac{p(\mathbf{x}_k | \mathbf{h}_k; \Omega) p(\mathbf{x}_k | \mathbf{s}_{1:K}, \theta^{(r)})}{p(\mathbf{x}_k | \mathbf{s}_{1:K}, \theta^{(r)})} d\mathbf{x}_k \\ &= \sum_{k=1}^K \int p(\mathbf{x}_k | \mathbf{s}_{1:K}, \theta^{(r)}) \log \frac{p(\mathbf{x}_k | \mathbf{h}_k; \Omega)}{p(\mathbf{x}_k | \mathbf{s}_{1:K}, \theta^{(r)})} + \int p(\mathbf{x}_k | \mathbf{s}_{1:K}, \theta^{(r)}) \log p(\mathbf{x}_k | \mathbf{s}_{1:K}, \theta^{(r)}) d\mathbf{x}_k \end{aligned} \quad (6)$$

where the first term is the negative of  $\mathbb{KL}$  divergence between the  $p(\mathbf{x}_k|\mathbf{s}_{1:K}, \boldsymbol{\theta}^{(r)})$  and  $p(\mathbf{x}_k|\mathbf{h}_k; \boldsymbol{\Omega})$ , and the second term is the negative of the posterior distribution entropy  $\mathbf{x}_k$  given the whole observations parameters estimated from the previous iteration of the EM. Now, we can rewrite  $Q$  as

$$Q(\boldsymbol{\theta}|\boldsymbol{\theta}^{(r)}) = \mathbb{E}_K[\log p(\mathbf{x}_0; \boldsymbol{\omega}_0) + \sum_{k=1}^K \log p(\mathbf{x}_k|\mathbf{x}_{k-1}; \boldsymbol{\omega}) +$$

$$\sum_{k=1}^K \log p(\mathbf{x}_k|\mathbf{s}_k, \mathbf{h}_k; \boldsymbol{\Omega})] + \sum_{k=1}^K \mathbb{KL}(p(\mathbf{x}_k|\mathbf{s}_{1:K}, \boldsymbol{\theta}^{(r)}) \| p(\mathbf{x}_k|\mathbf{h}_k; \boldsymbol{\Omega})) + \mathbb{H}(p(\mathbf{x}_k|\mathbf{s}_{1:K}, \boldsymbol{\theta}^{(r)})) \quad (7)$$

The last two terms in equation 7 are positive; thus, a lower bound for  $Q$  is the expectation over the state-transition and prediction process likelihood functions without taking the  $\mathbb{KL}$  and  $\mathbb{H}$  into account. This bound is unacceptable given it pushes the model parameter estimation in a favor of a prediction process with a long history term and possibly without incorporating the current observation, e.g non-informative about  $\mathbf{x}_k$ . If this is the case, the likelihood function, the first term in equation 1, becomes non-informative. On the other hand, the  $\mathbb{KL}$  reaches its maximum when the prediction process is only a function of the current observation, e.g.  $p(\mathbf{x}_k|\mathbf{h}_k; \boldsymbol{\Omega})$  almost flat over the possible values of  $\mathbf{x}_k$ . This dynamics of  $\mathbb{KL}$  suggests that there is an optimal history length that not only contributes to a better prediction of the state but also pushes  $Q$  to a higher value. We can use a greedy solution to incorporate both  $\mathbb{KL}$  and  $\mathbb{H}$  terms in the parameter estimation. Algorithm 1 presents the greedy optimization. The idea is to build D4 models with different history terms, whilst the parameter optimization per each D4 model is done without considering  $\mathbb{KL}$  and  $\mathbb{H}$  terms in 7. The D4 with optimal history term is the model with the highest  $Q$  values when the  $\mathbb{KL}$  and  $\mathbb{H}$  terms are added. Note that, we can calculate  $\mathbb{KL}$  and  $\mathbb{H}$  numerically or using sampling techniques when the model parameters are known. The downside of this greedy solution is that it makes the optimization computationally exhaustive. We discussed that the  $\mathbb{KL}$  divergence values sweep as that length of history term changes, where its maximum happens when the prediction process is not a function of history term. When the prediction process is not a function of history term; the  $\mathbb{KL}$  divergence can be approximated by negative of  $\mathbb{H}$  plus a constant term where the constant term represent negative of log of intensity of the prediction process over possible values of the state. The sum of  $\mathbb{KL}$  divergence plus the entropy will be a positive number that we want to maximize, therefore we want to maximize log of prediction process intensity. Note that the entropy term is only a function of the previous estimation of the model parameter; however, it provides a baseline for the  $\mathbb{KL}$  divergence. We assume the sum of the  $\mathbb{KL}$  plus  $\mathbb{H}$  should be larger than a pre-set positive threshold. With this assumption, we can approach our parameter optimization of  $Q$  from a regularization perspective. We define the regularization term by  $(\mathbb{KL}(p(\mathbf{x}_k|\mathbf{s}_{1:K}, \boldsymbol{\theta}^{(r)}) \| p(\mathbf{x}_k|\mathbf{h}_k; \boldsymbol{\Omega})) + \mathbb{H}(p(\mathbf{x}_k|\mathbf{s}_{1:K}, \boldsymbol{\theta}^{(r)})))^2$ , which can incorporate history length identification as part of the model training. Therefore, we can define the lower bound for the objective function as

---

**Algorithm 1** Greedy optimization of D4 model parameters
 

---

Set  $\mathbf{h}'_k \leftarrow \emptyset, l = 0, \mathbf{Q}^l \leftarrow 0$   
**do**  
    $l = l + 1$   
    $\mathbf{Q}^{max} \leftarrow \mathbf{Q}^l, \mathbf{h}_k \leftarrow \{\mathbf{s}_{k-l}, \mathbf{h}_k\}$   
   Initialize model parameters,  $\mathbb{E}_K[\cdot] \leftarrow 0$   
   **do**  
      $\mathbb{E}_K^{max}[\cdot] \leftarrow \mathbb{E}_K[\cdot]$   
     Run filter solution by equation 1  
     Run filter Smoother by equation 10  
     Draw sample trajectories for  $\mathbf{x}_k$  by equation 11  
     Find  $\theta$  that maximizes  $\mathbb{E}_K[\cdot]$  term of the equation 7  
   **while**  $\mathbb{E}_K[\cdot] > \mathbb{E}_K^{max}[\cdot]$   
    $\mathbf{Q}^l \leftarrow \mathbb{E}_K^{max}[\cdot] + \sum_{k=1}^K \mathbb{KL}(\cdot) + \mathbb{H}(\cdot)$   
**while**  $\mathbf{Q}^l > \mathbf{Q}^{max}$   
 Return the model associated with  $\mathbf{Q}^{max}$

---



---

**Algorithm 2** Regularized optimization of D4 model parameters
 

---

1: Set  $l \gg 1, \mathbf{h}_k \leftarrow \{\mathbf{s}_{k-l:k-1}\}, \lambda \geq 0, \mathbf{Q}^l \leftarrow 0$   
 2: Initialize model parameters  
 3: **do**  
    $\mathbf{Q}^{max} \leftarrow \mathbf{Q}^l$   
   Run filter solution by equation 1  
   Run filter Smoother by equation 10,  
   Draw sample trajectories for  $\mathbf{x}_k$  by equation 11  
   Find  $\theta$  that maximizes the  $\mathbf{Q}^l$  in equation 8  
 9: **while**  $\mathbf{Q}^l > \mathbf{Q}^{max}$   
 10: Return the model associated with  $\mathbf{Q}^{max}$

---

$$\begin{aligned} \mathbf{Q}(\theta|\theta^{(r)}) \geq & \mathbb{E}_K[\log p(\mathbf{x}_0; \omega_0) + \sum_{k=1}^K \log p(\mathbf{x}_k|\mathbf{x}_{k-1}; \omega) + \sum_{k=1}^K \log p(\mathbf{x}_k|\mathbf{s}_k, \mathbf{h}_k; \Omega)] \\ & - \lambda \sum_{k=1}^K (\mathbb{KL}(p(\mathbf{x}_k|\mathbf{s}_{1:K}, \theta^{(r)}) \| p(\mathbf{x}_k|\mathbf{h}_k; \Omega)) + \mathbb{H}(p(\mathbf{x}_k|\mathbf{s}_{1:K}, \theta^{(r)})))^2 \end{aligned} \quad (8)$$

where the multiplier  $\lambda \geq 0$  is the regularization coefficient that puts implicit pressure to shrink history length. We can use a stochastic gradient ascent solution to find this lower bound; thus, we require to find gradients of different terms of  $\mathbf{Q}$  respect to the model-free parameters. We can calculate  $\nabla \mathbf{Q}(\theta|\theta^{(r)})_{\Omega}$  by

$$\begin{aligned} \nabla \mathbf{Q}(\theta|\theta^{(r)})_{\Omega} = & \sum_{k=1}^K \frac{\nabla_{\Omega} p(\mathbf{x}_k|\mathbf{s}_k, \mathbf{h}_k; \Omega)}{p(\mathbf{x}_k|\mathbf{s}_k, \mathbf{h}_k; \Omega)} - 2\lambda \sum_{k=1}^K \int p(\mathbf{x}_k|\mathbf{s}_{1:K}, \theta^{(r)}) \left( \frac{\nabla_{\Omega} p(\mathbf{x}_k|\mathbf{h}_k; \Omega)}{p(\mathbf{x}_k|\mathbf{h}_k; \Omega)} \right) d\mathbf{x}_k \times \\ & (\mathbb{KL}(p(\mathbf{x}_k|\mathbf{s}_{1:K}, \theta^{(r)}) \| p(\mathbf{x}_k|\mathbf{h}_k; \Omega)) + \mathbb{H}(p(\mathbf{x}_k|\mathbf{s}_{1:K}, \theta^{(r)}))) \end{aligned} \quad (9)$$

See more details in appendix A. Given equation 9, we can optimize the  $\Omega$  using a stochastic backpropagation similar to the ones proposed for variational autoencoder models [15]. Algorithm 2 presents learning for D4 using stochastic backpropagation. So far, we assumed that  $\mathbf{x}_k$  is unobserved, when  $\mathbf{x}_k$  is known in the training dataset, the learning procedure follows the same steps where  $\mathbb{E}_K$  is replaced by the observed trajectory of the state.

## 2.2 Smoother estimation of the state, and sampling from the state posterior

To be able to do model parameters optimization efficiently, we use a smoother on the posterior density [20]. The smoother update equation begins with the filter solution at time index  $K$  at the end of the interval and proceeds backward from index  $K$  to index 1. The smoother is defined by

$$p(\mathbf{x}_k|\mathbf{s}_{1,\dots,K}) = p(\mathbf{x}_k|\mathbf{s}_{1,\dots,k}) \int \frac{p(\mathbf{x}_{k+1}|\mathbf{x}_k)p(\mathbf{x}_{k+1}|\mathbf{s}_{1,\dots,K})}{p(\mathbf{x}_{k+1}|\mathbf{s}_{1,\dots,k})} d\mathbf{x}_{k+1} \quad (10)$$

The smoother computes the posterior distribution of the state at time index  $k$  given all of the observed data through time  $K$ . Now we are able to use a sampling method to optimize the prediction and state transition models' parameters using the lower bound described in equation 8. To draw samples from the state trajectory, we can use the conditional distribution of  $\mathbf{s}_k$  given  $\mathbf{x}_{k+1}$ , and  $\mathbf{s}_{1:K}$ . This distribution can be computed by [20]

$$p(\mathbf{x}_k|\mathbf{x}_{k+1}, \mathbf{s}_{1:K}) = p(\mathbf{x}_{k+1}|\mathbf{x}_k) \times \frac{p(\mathbf{x}_k|\mathbf{s}_{1:k})}{p(\mathbf{x}_{k+1}|\mathbf{s}_{1:k})} \quad (11)$$

To draw a trajectory of state posterior distribution from  $k = 1$  to  $K$ , we draw a sample from  $p(x_K | s_{1:K})$ , which is calculated by the equation 10. We then recursively draw samples from equation 11 for time steps  $K - 1$  to 1. In cases, where the state is high-dimensional and computing the integrals in the filter and smoother equations using numerical methods becomes computationally expensive, we can use sequential MCMC methods, otherwise known as particle filters [8, 9].

### 2.3 Simulation Dataset

We generate the simulation dataset by assuming the state of interest,  $x_k$ , is a one-dimensional random walk defined by  $P(x_k | x_{k-1}) \sim N(ax_{k-1} + b, \sigma_x^2)$ , where  $a$  is the state transition and  $b$  is the bias coefficient for the random walk with a normal additive noise with a standard deviation of  $\sigma_x$ . Using the state, we then generate a 20-dimensional time-series signal with a conditional distribution defined by

$$P(s_k | x_k) \sim N(\mathbf{g}(x_k, x_{k-1}, \dots, x_{k-l_m}), \Sigma_s) \quad (12)$$

where  $\mathbf{g}(\cdot)$  is a 20 dimensional vector of non-linear functions, like tanh, and cosine, with an argument defined by a subset of state process at the current and previous time points. The  $l_m$  is the maximum number of data points used in creating  $\mathbf{g}(\cdot)$  function. For each channel of data, we pick a  $l$  uniformly from 0 to  $l_m$  randomly, which is used for the data generation. For example, in our simulation, the  $g_1$  function corresponding to the first element of  $\mathbf{g}$ , is a  $\tanh(\cdot)$  with the argument to be  $x_k + 0.8x_{k-1} + 0.6 * x_{k-2} + 0.4 * x_{k-3} + 0.2 * x_{k-4}$ .  $\Sigma_s$  is the stationary covariance matrix with size  $20 \times 20$ .  $\Sigma_s$ 's non-diagonal terms are non-zeros, implying observations across channels are correlated. In our simulation, we picked  $a = .9$ ,  $b = 0$ , and  $\sigma_x = 0.1$ . We generate the data for 1000 data points. Figure 2.A shows a trajectory of the state and observed data. Our simulation data has a complex observation along with a low-dimensional state process; this setting was purposefully picked to demonstrate D4 prediction power and build a clear comparison across models. We also show the D4 model performance in neural data which can probe other aspects of the proposed framework and its training process.

## 3 Results

To demonstrate and compare DDD and D4 models capability in inferring the underlying state ( $x_k$ ), we start with the simulation data described in section 2.3. We assume the state process is defined by

$$x_k = \alpha x_{k-1} + \beta + w_k, \quad w_k \sim N(0, \sigma_x^2) \quad (13)$$

where  $\sigma_x$  is the standard deviation of the state variable.

- For DDD, we assume the prediction process is a linear model with an additive Gaussian noise,  $p(x_k | s_k, \mathbf{h}_k, \Omega) \sim N(\sum \Omega_1 \odot s_k + \Omega_2 \odot \mathbf{h}_k, \sigma_s^2)$ . Where  $\Omega_1$  and  $\Omega_2$  are the prediction process parameter sets associated to the current observation and the history; respectively.
- For D4, we assume the prediction process is a DNN model with additive Gaussian noise,  $p(x_k | s_k, \mathbf{h}_k, \Omega) \sim N(\mu_\Omega(s_k, \mathbf{h}_k), \sigma_\Omega(s_k, \mathbf{h}_k))$ . Where  $\mu_\Omega(s_k, \mathbf{h}_k)$  and  $\sigma_\Omega(s_k, \mathbf{h}_k)$  are the mean and standard deviation of the Gaussian noise which both are nonlinear functions of the current,  $s_k$ , and the history,  $\mathbf{h}_k$ .

Given the simulation data, we are trying to simultaneously update the state transition and prediction process parameters that maximizes the  $Q$  given  $s_k$ . It is worth mentioning that  $s_k$  is a vector of length 20, and  $\mathbf{h}_k$  length 20 times the size of the history term. Figure 2.B shows the  $Q$  value as a function of history term for both DDD and D4 models. Using Algorithm 1, the optimal length of the history term is 5, whilst D4 has a higher  $Q$  value than the DDD model. Figure 2.C shows the  $Q$  values as function of  $\lambda$  for both DDD and D4 models. A larger  $\lambda$  penalizes the history term more which corresponds to a drop in the  $Q$  values as  $\lambda$  grows. Optimal values of  $\lambda$  for DDD and D4 models are 0.67 and 0.81; this is expected, as we expect larger penalization for the D4 given a higher number of free parameters. In Algorithm 2, we start with a fixed and reasonably large history term; the history term in both models was set to last 20-time points. We used mean-squared-error (MSE) and correlation coefficient (CC) to measure the accuracy of the D4 models in predicting state [4]. Figure 2.D shows these measures for both models while trained using Algorithms 1 and 2 with 2-fold cross-validation. The result suggests that the D4 model trained using Algorithm 2 gives the highest performance. This

is not surprising; however, this performance has been maintained without observing an overfitting problem. Figure 2.E shows D4 model prediction in the test and training set (here we considered 50% of data for training and the remaining 50% for testing). The  $Q$  curve in Figure 2.B along with our prediction results suggest that DDDs benefit from the history term. Appendix B shows the prediction result for the DDD along with GRU-RNN and SSM; among all these models, the D4 again maintains the highest performance.

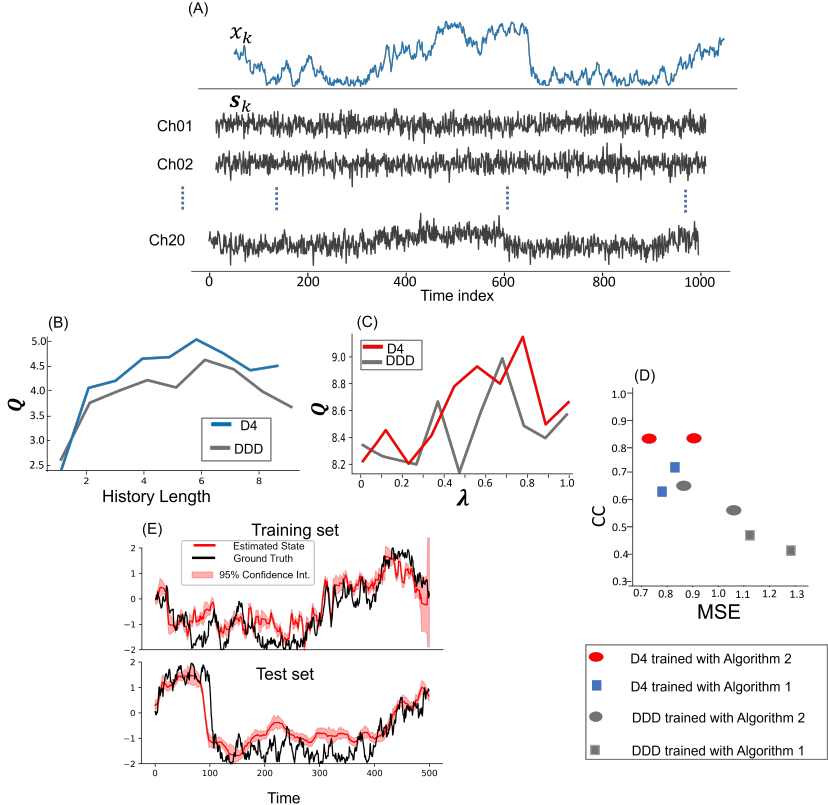


Figure 2: The D4 modeling results for the simulated data. A) A sample of simulated data. B)  $Q$  function values as a function of history term using Algorithm 1. C)  $Q$  function values for different regularization terms,  $\lambda$ , using Algorithm 2. D) 2-fold cross-validated correlation coefficient (CC) and mean-squared error (MSE) for DDD and D4 models with the proposed algorithms. The D4 trained with Algorithm 2 attains the highest performance with 2-fold cross-validation. E) The decoding result (smoother) using the D4 in the training and test sets.

### 3.1 D4 comparison with traditional time-series decoders

We also compared the D4 model against the current time series decoder models, we compare its result with traditional SSMs[22] and GRU-RNNs[5]. We do that by considering similar prediction processes described in previous section and selecting proper functions for  $\mu_{\Omega}(s_k, h_k)$  and  $\sigma_{\Omega}(s_k, h_k)$  to represent each model. We try these three models on the simulation dataset (see appendix B for its results), described before, and on the position decoding problem from multi-electrode recorded neural activity of a rat while it forages a W-shaped maze for food[19]. We measured the performance of the decoder models using mean squared error (MSE), mean absolute error (MAE) [4], and the 95% highest posterior density region (HPD) metrics[25]. In this problem, we seek to decode the 2-D movement trajectory of a rat traversing through a W-shaped maze from the ensemble spiking activity of 62 hippocampal place cells. We define the state variable  $c_k = (x_k, y_k)$  where  $x_k$  and  $y_k$  represents the rat coordinates in the 2D spaces. The neural data were recorded from 62 place cells in the CA1 and CA2 regions of the hippocampus brain area of a rat. Figure 3.A shows the spiking activity of these 62 units,  $s_k \in \mathbb{R}^{62^2}$ . For the state process, we use a 2-D random walk model. For

the prediction process, we assume that the noise process follows a 2-dimensional normal distribution. As a result, the prediction process is a multi-variate regression model for  $c_k$ s. For D4, we can assume the joint probability model can be written as the product of two predictor models,

$$P(c_k | s_k, h_k) = P(x_k | s_k, h_k, y_k; \Omega_x) \times P(y_k | s_k, h_k; \Omega_y) \quad (14)$$

where each predictor model can be a DNN. Similar to the simulation data problem, we use a normal distribution where the mean and variance are a function of the current spiking activity of 62 cells and their spiking history. Along with D4, we also build SMM, explained in [22, 18] and GRU-RNN [5] models. Figure 3 Shows their result. Among these models, D4 gives a significantly better 95% HPD compared to the SSM model. Note that this comparison is not possible for GRU-RNN, as its output is deterministic. The D4 model outperforms both SSM and GRU-RNN with regard to MSE, especially in the X-direction where the long-term temporal information is playing a significant role. We think D4 performance precedes other models given it incorporates different temporal at moderate and slower timescales in its prediction of the rat position. In fact, this is aligned with the physiological of cells where their spiking activity is dependent on their previous spiking. This mechanism is not present in RNN, as in RNN, a single state that is governed by parameterized gates to reach a trade-off between long-term and short-term dynamics. As the result, the D4 model has a better performance in the X-direction. The other attribute of D4 is immunity to overfitting. As it can be seen in Figure 3.I-J, the variation of D4 decoding results between training and test performance is significantly less than the GRU-RNN model. We think both the state process and regularized process in picking history terms play roles in decoding stability. This result suggests we can utilize the D4 in modeling problems with a smaller dataset, where GRU-RNN might face over-fitting issues.

## 4 Discussion

In this research, we introduced a new modeling solution to characterize multi-variate time-series data. We call the solution D4 model, which incorporates DNN into the recently proposed modeling solution called direct discriminative decoder, DDD. We revisited the inference solution using D4 and developed learning algorithms for the D4 model. We further demonstrated its solution in simulation and real datasets, where its performance preceded RNN, SSM, and DDD models. The DDD is a variant of the SSM, in which the conditional distribution of the observation is replaced by a discriminative process. The D4 inherits attributes of DDD, while it provides higher expressive power for its prediction process by using DNNs. In SSMs, the inference process combines two sources of information at different time scales: a) fast, which incorporates the information carried at the current time observation, and b) slow, which incorporates the information on how the state evolves over a longer time scale. The DDD hypothesis is if the fast time scale is replaced by an intermediate time scale, we can better characterize time-series data. If this hypothesis holds, we can even push the DDD utility by using DNN as its prediction process. The results in both simulation and hippocampus place cells support this claim; we reach higher  $Q$  values along with a better MSE and CC for D4 compared to DDD. RNN and GRU have been successfully applied in characterizing time-series data where the observed signals reflect changes in an underlying latent process. RNN and GRU are mainly agnostic to the state process and search for the optimal history term through exploration or a gating mechanism. Instead, in the D4, the search from the history term is guided by the state process which is added to the model. As a result, in the worst case, we expect D4 performance to be on par with RNN and GRU. The simulation results show that D4 performance precedes RNNs; more importantly, D4 shows a less discrepancy in its performance for the test and training datasets. Thus, the D4 shows not only a higher prediction accuracy but also a more robust prediction. In the discriminative processes, the focus is on the performance, not the probing underlying mechanism of how the data is generated. The D4 lives somewhere between generative and discriminative domains; thus, the D4 provides an etiological interpretation of our findings. This is important in many fields and in particular neuroscience. The Bayesian approach in formulating the D4 lets us add other observations to the model like those being used in SSMs. In other words, we can have both generative and discriminative observation processes. This is important in neuroscience as we have other bio-physiological correlated like reaction time (RT) with a simpler dynamic and can be embedded in the pipeline. The problem presented here has relatively simple state processes, which are defined by random-walk models. The advantage of the random walk model is that they maintain continuity of the state, whilst they do not impose any further information like drift and complex dynamics across state variables. Practically, the D4 training is applicable to more complex state processes. Note that, the state process free parameters are present in the regularization term, and the choice of their free parameter will influence the history term of the

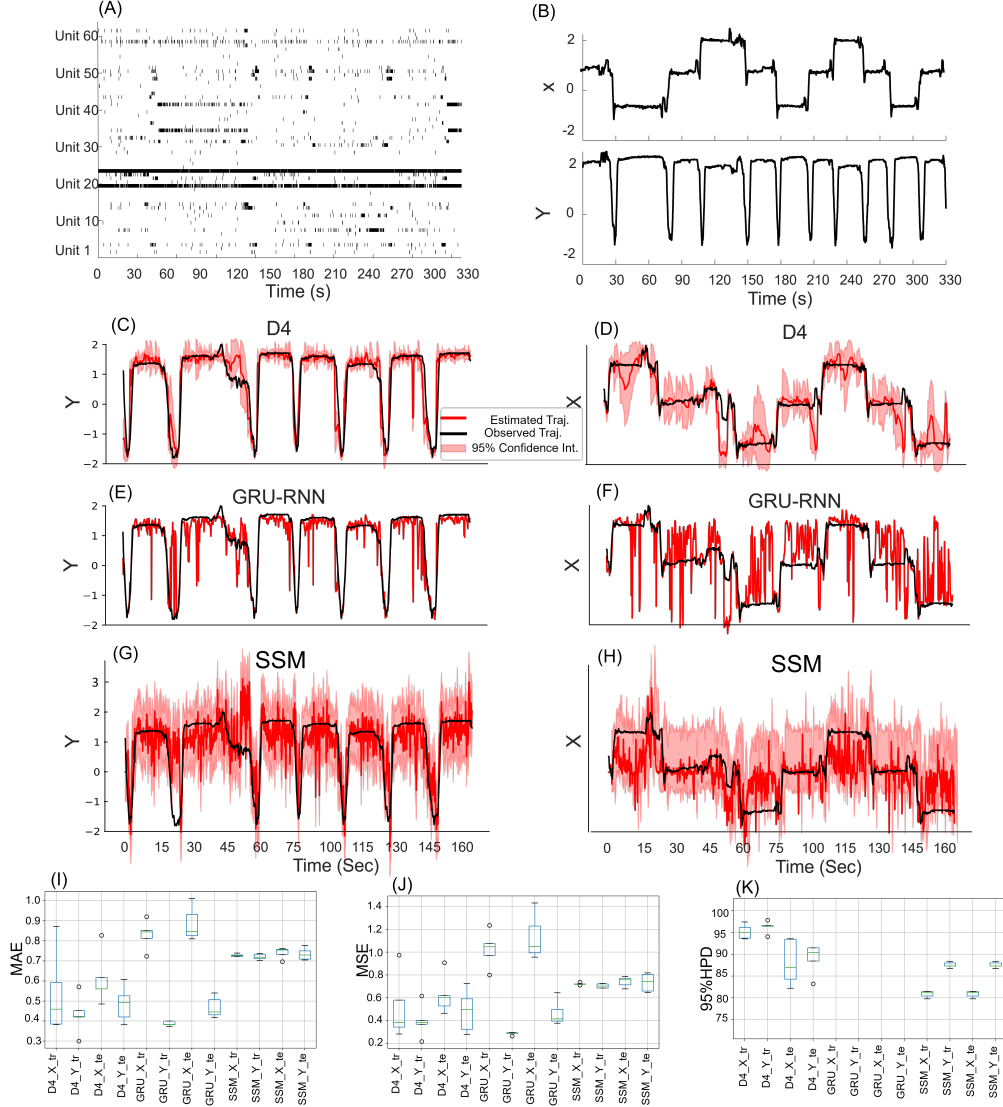


Figure 3: Decoding of the rat trajectory from its hippocampus neural activity using D4, SSM, and GRU-RNN. A) an example of spiking activity of 62 cells recorded for 330 seconds while the rat is traversing in a W-shaped maze dataset. B) The rat observed position X&Y-directions during the 330 seconds time. C) The D4 decoding result for Y-axis. D) The D4 decoding result for X-axis. E) The GRU-RNN decoding result for Y-axis. F) The GRU-RNN decoding result for X-axis. G) The SSM decoding result for Y-axis. H) The SSM decoding result for X-axis. We find the state transition parameter ( $\sigma_x$ ) of the SSM empirically from the training set. I) The MAE results for D4, SSM, and GRU-RNN for the x- and y-axis. J) The MSE results for D4, SSM, and RNN for the x- and y-axis. K) The 95% highest posterior density (HPD) interval for D4, SSM, and RNN for the x- and y-axis. The decoder models are trained using the first 80% of data and the test is performed for the last 20% data.

prediction process. When the complexity of training and calculating the gradient of the regularization term grows, we can use the greedy training algorithm (Algorithm 1). It is worth noting that the inference will be the same as it is defined in equation 1. We used a numerical approach to solve the learning step. To do this, we draw samples from the trajectory given the filter and a smoother solution. We calculate the filter and the smoother solution has numerically given the dimension of the state; we then draw samples from the trajectory which can be used in the estimation of the model parameters. When the dimension of the state grows, we can move to an MCMC solution to find the

filter and smoother solution, which provide samples needed for the optimization. Here, our focus was on motivating the D4 model and demonstrating its learning process. Our future research focuses on deploying the solution to a much larger hippocampus dataset which includes about 2000 channels of spiking activity. Furthermore, we are interested in studying hippocampus ripple events where there is no observation of the latent process, or projected movement directory, and we require to connect observed instances of the data to those which lack the state. In the development of the D4, we took an ML approach to assess and compare model performance. We use MSE, CC, and  $Q$  value to show whether a model performance precedes others or not. We can approach the model comparison from a goodness-of-fit perspective to check how well the inferred states and model parameters represent the observed dataset. This will be another scope of our future research.

## Broader Impact

The state-of-art solution for decoding through high-dimensional time-series data and those with a complex dynamic are heavily dependent on discriminative models like DNN and RNNs. Despite a high expressive power, these models' performance decreases as we move from a static to dynamic inference even when the underlying latent process is low dimensional with reasonably predictable dynamics. The deterministic approach to the inference which is practiced in the majority of these models further limits their inference reliability and introduces high variance in the prediction. The remedy being practiced is relying on larger training sets along with growing the model complexity. Whilst this might work in problems that are mainly focused on prediction accuracy and access to a larger dataset is possible. When the scientific pursuit is on the inference and creating a larger dataset is not practical, we require solutions that can inherit attributes of the aforementioned solution whilst they are not data greedy. The D4 solution introduced in this research shows a decoding performance that precedes RNN and DNNs, with less variance in its prediction. The D4 model provides a principle solution to embed the state process information in DNN and RNN models; thus, its inference can have more ethological interpretation. The inference in the D4 is probabilistic rather than deterministic; this utility provides further clarity on the decoding step which is necessary for the scientific pursuit of what the data represents. The D4 application is not limited to neuroscience data, and it can be applied to a broad range of applications including NLP, and ASR. The D4 is scalable, and it can easily deal with the growth in the dimensional of the time-series data without changing the pipeline.

## 5 Acknowledgments and Disclosure of Funding

This work was supported by Dr. Lankarany's NSERC Fund (RGPIN-2020-05868) and MITACS Accelerate (IT19240).

## References

- [1] Masanao Aoki. *State space modeling of time series*. Springer Science & Business Media, 2013.
- [2] Emery N Brown, Loren M Frank, Dengda Tang, Michael C Quirk, and Matthew A Wilson. A statistical paradigm for neural spike train decoding applied to position prediction from ensemble firing patterns of rat hippocampal place cells. *Journal of Neuroscience*, 18(18):7411–7425, 1998.
- [3] Michael C Burkhart, David M Brandman, Brian Franco, Leigh R Hochberg, and Matthew T Harrison. The discriminative kalman filter for bayesian filtering with nonlinear and nongaussian observation models. *Neural Computation*, 32(5):969–1017, 2020.
- [4] Tianfeng Chai and Roland R Draxler. Root mean square error (rmse) or mean absolute error (mae)?—arguments against avoiding rmse in the literature. *Geoscientific model development*, 7(3):1247–1250, 2014.
- [5] Junyoung Chung, Caglar Gulcehre, KyungHyun Cho, and Yoshua Bengio. Empirical evaluation of gated recurrent neural networks on sequence modeling. *arXiv preprint arXiv:1412.3555*, 2014.

- [6] Ronan Collobert and Jason Weston. A unified architecture for natural language processing: Deep neural networks with multitask learning. In *Proceedings of the 25th international conference on Machine learning*, pages 160–167, 2008.
- [7] Arthur P Dempster, Nan M Laird, and Donald B Rubin. Maximum likelihood from incomplete data via the em algorithm. *Journal of the Royal Statistical Society: Series B (Methodological)*, 39(1):1–22, 1977.
- [8] Arnaud Doucet, Simon Godsill, and Christophe Andrieu. On sequential monte carlo sampling methods for bayesian filtering. *Statistics and computing*, 10(3):197–208, 2000.
- [9] Arnaud Doucet, Adam M Johansen, et al. A tutorial on particle filtering and smoothing: Fifteen years later. *Handbook of nonlinear filtering*, 12(656-704):3, 2009.
- [10] James Durbin and Siem Jan Koopman. *Time series analysis by state space methods*, volume 38. OUP Oxford, 2012.
- [11] Uri T Eden, Loren M Frank, Riccardo Barbieri, Victor Solo, and Emery N Brown. Dynamic analysis of neural encoding by point process adaptive filtering. *Neural computation*, 16(5):971–998, 2004.
- [12] Reza Saadati Fard, Kensuke Arai, Uri T Eden, Emery N Brown, and Ali Yousefi. Analysis of distributed neural synchrony through state-space coherence analysis. *bioRxiv*, 2020.
- [13] Sepp Hochreiter and Jürgen Schmidhuber. Long short-term memory. *Neural computation*, 9(8):1735–1780, 1997.
- [14] Jack Karush. On the chapman-kolmogorov equation. *The Annals of Mathematical Statistics*, 32(4):1333–1337, 1961.
- [15] Diederik P Kingma and Max Welling. Auto-encoding variational bayes. *arXiv preprint arXiv:1312.6114*, 2013.
- [16] Peter Molenaar. A dynamic factor model for the analysis of multivariate time series. *Psychometrika*, 50(2):181–202, 1985.
- [17] Mohammad R Rezaei, Anna K Gillespie, Jennifer A Guidera, Behzad Nazari, Saeid Sadri, Loren M Frank, Uri T Eden, and Ali Yousefi. A comparison study of point-process filter and deep learning performance in estimating rat position using an ensemble of place cells. In *2018 40th Annual International Conference of the IEEE Engineering in Medicine and Biology Society (EMBC)*, pages 4732–4735. IEEE, 2018.
- [18] Mohammad R. Rezaei, Alex E. Hadjinicolaou, Sydney S. Cash, Uri T. Eden, and Ali Yousefi. Direct Discriminative Decoder Models for Analysis of High-Dimensional Dynamical Neural Data. *Neural Computation*, pages 1–36, 03 2022.
- [19] Mohammad Reza Rezaei, Kensuke Arai, Loren M Frank, Uri T Eden, and Ali Yousefi. Real-time point process filter for multidimensional decoding problems using mixture models. *Journal of Neuroscience Methods*, 348:109006, 2021.
- [20] Simo Särkkä. *Bayesian filtering and smoothing*. Number 3. Cambridge University Press, 2013.
- [21] Ian Tenney, Dipanjan Das, and Ellie Pavlick. Bert rediscovered the classical nlp pipeline. *arXiv preprint arXiv:1905.05950*, 2019.
- [22] Wilson Truccolo, Uri T Eden, Matthew R Fellows, John P Donoghue, and Emery N Brown. A point process framework for relating neural spiking activity to spiking history, neural ensemble, and extrinsic covariate effects. *Journal of neurophysiology*, 93(2):1074–1089, 2005.
- [23] Aäron Van Den Oord, Sander Dieleman, Heiga Zen, Karen Simonyan, Oriol Vinyals, Alex Graves, Nal Kalchbrenner, Andrew W Senior, and Koray Kavukcuoglu. Wavenet: A generative model for raw audio. *SSW*, 125:2, 2016.
- [24] Eric A Wan and Alex T Nelson. Dual extended kalman filter methods. *Kalman filtering and neural networks*, 123, 2001.

- [25] Weixin Yao and Bruce G Lindsay. Bayesian mixture labeling by highest posterior density. *Journal of the American Statistical Association*, 104(486):758–767, 2009.
- [26] Ali Yousefi, Reza Saadati Fard, Uri T Eden, and Emery N Brown. State-space global coherence to estimate the spatio-temporal dynamics of the coordinated brain activity. In *2019 41st Annual International Conference of the IEEE Engineering in Medicine and Biology Society (EMBC)*, pages 5794–5798. IEEE, 2019.
- [27] Qingchen Zhang, Laurence T Yang, Zhikui Chen, and Peng Li. A survey on deep learning for big data. *Information Fusion*, 42:146–157, 2018.

## 6 Calculating the gradient of the KL with respect to the prediction process of the D4 model

The gradient of  $Q$  is defined by

$$\begin{aligned} \nabla Q(\theta|\theta^{(r)})_{\Omega} &= \sum_{k=1}^K \nabla_{\Omega} \log p(\mathbf{x}_k | \mathbf{s}_k, \mathbf{h}_k; \Omega) - 2\lambda \sum_{k=1}^K \nabla_{\Omega} \mathbb{KL}(p(\mathbf{x}_k | \mathbf{s}_{1:K}, \theta^{(r)}) \| p(\mathbf{x}_k | \mathbf{h}_k; \Omega)) \times \\ &\quad (\mathbb{KL}(p(\mathbf{x}_k | \mathbf{s}_{1:K}, \theta^{(r)}) \| p(\mathbf{x}_k | \mathbf{h}_k; \Omega)) + \mathbb{H}(p(\mathbf{x}_k | \mathbf{s}_{1:K}, \theta^{(r)}))) \end{aligned} \quad (15)$$

The first term is gradient of the prediction process and it can be calculated through the backpropagation technique. The second term in equation 15 can be calculated as

$$\begin{aligned} \nabla_{\Omega} \mathbb{KL}(p(\mathbf{x}_k | \mathbf{s}_{1:K}, \theta^{(r)}) \| p(\mathbf{x}_k | \mathbf{h}_k; \Omega)) &= \\ \nabla_{\Omega} \int p(\mathbf{x}_k | \mathbf{s}_{1:K}, \theta^{(r)}) \log \frac{p(\mathbf{x}_k | \mathbf{s}_{1:K}, \theta^{(r)})}{p(\mathbf{x}_k | \mathbf{h}_k; \Omega)} d\mathbf{x}_k &= \\ \int p(\mathbf{x}_k | \mathbf{s}_{1:K}, \theta^{(r)}) \nabla_{\Omega} \log \frac{p(\mathbf{x}_k | \mathbf{s}_{1:K}, \theta^{(r)})}{p(\mathbf{x}_k | \mathbf{h}_k; \Omega)} d\mathbf{x}_k &= \\ \int p(\mathbf{x}_k | \mathbf{s}_{1:K}, \theta^{(r)}) \nabla_{\Omega} \log p(\mathbf{x}_k | \mathbf{s}_{1:K}, \theta^{(r)}) d\mathbf{x}_k - \int p(\mathbf{x}_k | \mathbf{s}_{1:K}, \theta^{(r)}) \nabla_{\Omega} \log p(\mathbf{x}_k | \mathbf{h}_k; \Omega) d\mathbf{x}_k &= \\ - \int p(\mathbf{x}_k | \mathbf{s}_{1:K}, \theta^{(r)}) \nabla_{\Omega} \log p(\mathbf{x}_k | \mathbf{h}_k; \Omega) d\mathbf{x}_k &= \\ - \int p(\mathbf{x}_k | \mathbf{s}_{1:K}, \theta^{(r)}) \frac{\nabla_{\Omega} p(\mathbf{x}_k | \mathbf{h}_k; \Omega)}{p(\mathbf{x}_k | \mathbf{h}_k; \Omega)} d\mathbf{x}_k \end{aligned} \quad (16)$$

Given equations 15 and 16 we can write the gradient by

$$\begin{aligned} \nabla Q(\theta|\theta^{(r)})_{\Omega} &= \sum_{k=1}^K \frac{\nabla_{\Omega} p(\mathbf{x}_k | \mathbf{s}_k, \mathbf{h}_k; \Omega)}{p(\mathbf{x}_k | \mathbf{s}_k, \mathbf{h}_k; \Omega)} + 2\lambda \sum_{k=1}^K \int p(\mathbf{x}_k | \mathbf{s}_{1:K}, \theta^{(r)}) \frac{\nabla_{\Omega} p(\mathbf{x}_k | \mathbf{h}_k; \Omega)}{p(\mathbf{x}_k | \mathbf{h}_k; \Omega)} d\mathbf{x}_k \times \\ &\quad (\mathbb{KL}(p(\mathbf{x}_k | \mathbf{s}_{1:K}, \theta^{(r)}) \| p(\mathbf{x}_k | \mathbf{h}_k; \Omega)) + \mathbb{H}(p(\mathbf{x}_k | \mathbf{s}_{1:K}, \theta^{(r)}))) \end{aligned} \quad (17)$$

## 7 Further performance comparison in simulation data

Here, we tested SSM and GRU-RNN model decoding performance along with the D4. For the training, we assumed the state process is observed. This is because we needed the state for GRU-RNN training, and having the states, training of the SSM becomes simple. For SSM training, we can find the state and observation processes parameters using the MLE technique, if the state trajectory is known. Please note we already discussed how we can train the D4 model when the state is known. Figure 4 shows the D4, GRU-RNN, and SSMs decoding results on the simulation dataset. The D4 model MAE and MSE measures outperforms both SSM and GRU-RNN models on the test dataset. The D4 model also gives even a significantly better 95% HPD compared to the SSM model.

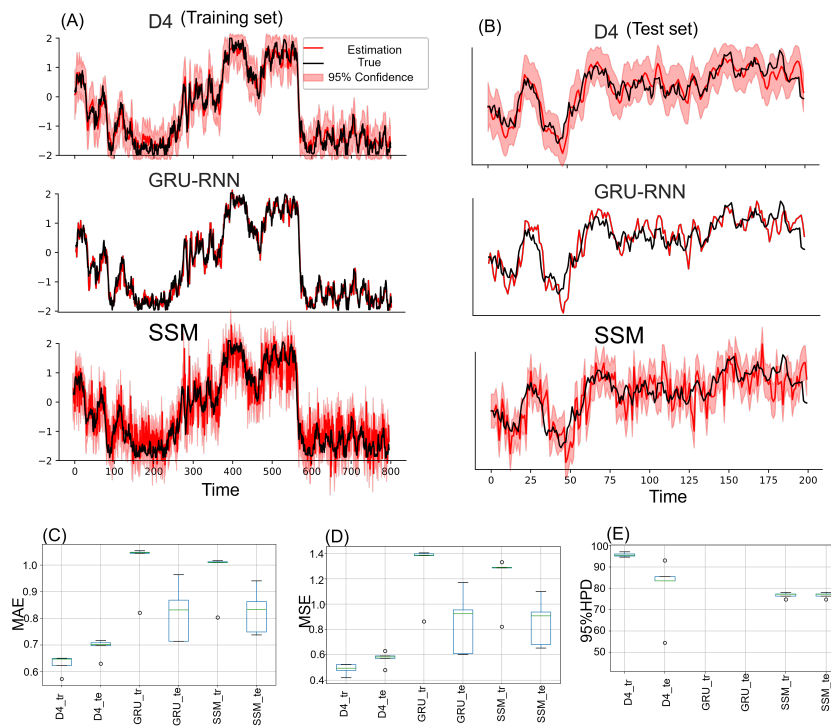


Figure 4: Decoding results for simulation dataset using D4, GRU-RNN, and SSM models. A) Decoding results for the training set. B) Decoding results for the test set. C) MAE. D) MSE. E) 95% HPD. Note that the GRU-RNN model has a deterministic output; as a result, there is no 95% HPD measure for the GRU-RNN model.